ISSN 1061-933X, Colloid Journal, 2024, Vol. 86, No. 5, pp. 780–790. © Pleiades Publishing, Ltd., 2024.

Control over Technological Parameters of Detonation Spraying for Producing Titanium Dioxide Coatings with Specified Wetting Properties

V. V. Sirota[a], S. E. Savotchenko[a, b, *], V. V. Strokova[a], D. S. Podgoronyi[a], S. V. Zaitsev[a], A. S. Churikov[a], and M. G. Kovaleva[c]

[a] *Shukhov Belgorod State Technological University, Belgorod, 308012 Russia*

[b] *Sergo Ordzhonikidze Russian State University for Geological Prospecting, Moscow, 117997 Russia*

[c] *Belgorod National Research University, Belgorod, 308015 Russia*

**e-mail: savotchenkose@mail.ru*

Received May 26, 2024; revised July 23, 2024; accepted July 23, 2024

Abstract—The water-repellent properties have been studied for the surface of a protective metal–ceramic coating based on titanium dioxide. It has been shown that the water-repellent properties of the coating surface can be efficiently changed by varying the technological parameters of spraying. When producing the coatings, technological parameters, such as the distance between a substrate and a detonation gun barrel (spraying distance) and the speed of barrel movement, have been varied. Regularities have been derived to relate the technological parameters of the detonation spraying of the coating and its contact angle. It has been found that, under certain conditions, the dependence of the contact angle on the spraying distance obeys a parabolic law. Parameters have been calculated for the phenomenological equation that adequately describes the observed parabolic dependence. The optimal values of the detonation spraying parameters necessary to achieve the maximum hydrophobicity of the produced coatings have been determined.

Keywords: titanium dioxide, metal–ceramic coatings, detonation spraying, hydrophobic properties, contact angle, wetting angle, spray distance, nozzle speed

DOI: 10.1134/S1061933X24600933

INTRODUCTION

Metal–ceramic composite coatings based on titanium dioxide (TiO_2) belong to the class of photocatalytic coatings [1]. They are produced by numerous technologies [2–6], among which the detonation spraying method [7–9] may be distinguished.

Many coatings are used to protect materials from various influences, including contamination. The protection can be achieved due to the capability of the coatings for self-cleaning from various contaminants owing to the photocatalytic properties [10]. When developing such coatings, the water-repellent properties of their surfaces play a decisive role [11]. Therefore, it is of importance to find the process regularities and determine the relations between the technological parameters of the detonation spraying of titanium dioxide coatings and the wetting properties of their surfaces.

Variations in the contact angle at the surface of a titanium dioxide coating make it possible to control its water-repellent properties [12, 13]. Therefore, there is a need to experimentally measure the contact angle of a liquid (e.g., water) at the surfaces of coatings obtained under different spraying conditions. Such experiments make it possible to find the relationship between the controllable parameters of spraying regimes and the water-repellent properties [14].

Despite the fact that the technologies for applying titanium dioxide coatings, including detonation spraying, are widely used, the influence of spraying parameters on the properties of the resulting coatings remains to be studied [15]. Recently, we presented the results of developing and studying titanium-dioxide-based composite photocatalytic coatings [16–18]. In that works, we studied the microstructure and phase composition of the coatings, as well as the photocatalysis kinetics. However, the water-repellent properties of such coatings have not been studied in the context of their relationship with spraying parameters. In this paper, we present the results of experimental studies that reveal the relationship between the parameters of the detonation spraying of coatings and the wetting properties of their surfaces.

Studying the behavior of the contact angles at coating surfaces formed under different conditions makes it possible to develop recommendations for controlling the water-repellent properties by varying the

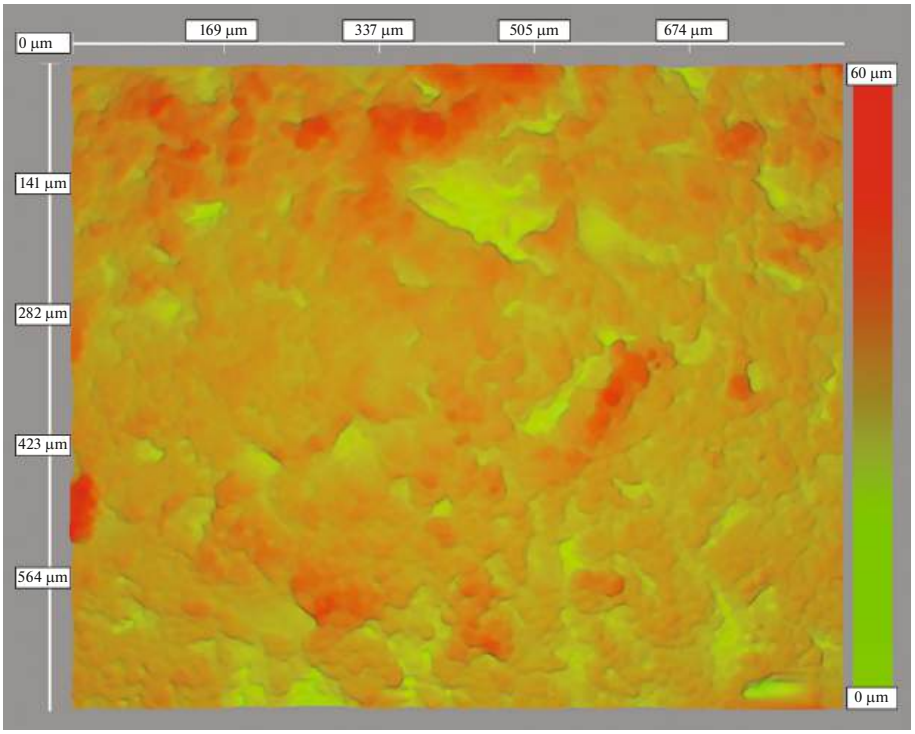

Fig. 1. Optical image of the substrate surface (height map).

technological parameters in the process of manufacturing self-cleaning metal–ceramic coatings with photocatalytic properties.

EXPERIMENTAL

Titanium powder of the PTN8-VT1.0 brand (Ltd. "Normin," Russia) was used for spraying. A fraction of 40–60 μm was separated from the powder by the sieve method. Before spraying, the powder was dried in an electric oven at a temperature of 200 ± 5°C for 60 min to reduce agglomeration and eliminate the possibility of coalescence during the detonation spraying process.

The substrates for the coating were prepared from steel of the St3 brand as square samples with sizes of 40 × 40 mm. The surfaces of the steel samples (substrates) were preliminarily degreased and sandblasted. The substrate surface roughness was determined using a Taylor-Hobson Surtronic 25 profilometer (Taylor Hobson Ltd, United Kingdom). After sandblasting, substrate surface roughness *Ra* was 3.50 ± 0.15 μm; the surface optical image is shown in Fig. 1 (height map) to visually display the morphology of the substrate surface.

The coatings were applied using a robotic detonation spraying complex (Ltd. IntelMashin, Russia). The layout and photographs of the detonation spraying setup can be found in [8, 16], respectively. The gas flow rate was measured with float flowmeters. The detonation device operating parameters unchangeable during the coating process are given in Table 1.

The coatings were formed under different regimes, in which the following parameters were varied: distances *d* (mm) between the detonation gun nozzle and a substrate (spraying distances) were 40, 50, 60, 70, and 80; speeds *s* (mm/min) of the detonation gun movement (nozzle speeds) were 400, 800, 1200, 1600, and 2000. Two passes were performed on each sample.

The contact angle, roughness, and profile were measured on the surfaces of coating samples obtained using combinations of each of the aforementioned values of spraying parameters. The surface profile and roughness of the coatings were measured in the visible field of an MT-24RF direct optical metallographic

Table 1. Constant spraying parameters (* and ** denote cylindrical and annular combustion chambers, respectively)

Consumption of combustible mixture components, m^3/h			Powder feed rate, g/h	Gun barrel length, mm	Gun nozzle diameter, mm
air	oxygen	propane			
1.3*/1.54**	2.44*/3.04**	0.56*/0.67**	800	300	16

microscope (SIAMS, China) using the SIAMS 800 software package (SIAMS, Russia). This software package has the function of constructing relief along secant focal planes. Measurement procedure was as follows: the function for constructing a 3D surface and the step size (μm) and the number of steps of lens displacements were selected. In our case, the movement was carried out over a distance of 300 μm with a step of 2 μm. A focused fragment of the image was automatically detected and used as a layer with a preset height counted by the number of steps. After the measurement was completed (a preset height was reached), a 3D surface was formed from the obtained layers.

The roughness was determined by constructing a grid of 15 × 15 lines (standard roughness determination function in the SIAMS 800). The relief was determined in the diagonal direction from corner to corner (a line was also constructed, which was an array of two columns: the height of the relief and the distance). The measurements of the relief and roughness were repeated five times for each sample, and their average value was taken as the result.

The contact angle was measured with a KRUSS DSA30E analyzer of distilled water droplet shape (KRUSS, Germany). This instrument was equipped with an automatic program-controlled dispenser. Distilled water was used as the test liquid. Droplet volume was 4 μL, and the time required for stabilization was 30 s. The instrument had a hardware–software complex for moving the syringe dosing the droplets. The general description of the process was as follows: the dosing syringe was installed at a basic distance from the sample (15 mm) to form a droplet. The droplet was formed in an automated mode at a rate of 2 μL/s. After a 4-μL droplet was formed, the dosing syringe was moved toward the sample at a speed of 100 mm/min. After the droplet touched the surface and the dosing syringe was brought to a distance of 1 mm from the sample, the syringe was removed from the sample at a speed of 100 mm/min and brought to the basic distance. The droplet fell onto the sample; then, the stabilization was waited for 30 s. The tests were carried out at a temperature of 25°C and a relative air humidity of about 50%. The measurements were repeated ten times, and the average value of the results was taken as the final contact angle.

In order to additionally investigate the relationship between the spraying distance and the diameter of the spray spot, large square samples 100 × 100 mm in sizes were prepared. The procedure for this series of the experiments was as follows: after the detonation setup was brought into the normal spraying regime, it was brought to the point of spraying the spot at a speed of 2000 mm/min, where the spraying was carried out for 5 s; then, the gun was moved to its initial position at a speed of 2000 mm/min.

RESULTS AND DISCUSSION

Since the detonation spraying is performed at a high temperature, a large fraction of titanium is oxidized during the formation of the coatings. The phase composition of the coatings produced by the detonation spraying using the same setup and the same starting raw materials was reported in our previous work [17], where electron microscopy images, as well as the results of the X-ray diffraction analysis, were presented. It can be stated that the total fraction of titanium dioxide in the forms of rutile and anatase is, on average, at least 50%; titanium oxide fraction is about 22%; and titanium fraction is at most 18%. Similar results were presented in [16]. These results agree with the data obtained by other authors [7–10], who reported that this technology of titanium powder spraying yielded rutile and anatase as the main fractions of a coating, with the ratio between them determining the photocatalytic properties of the coating.

Note that variable factors in the detonation spraying technology could be the rate of the powder consumption and the composition of the gas mixture (Table 1). However, previous studies [8, 16–18] have shown that these parameters predetermine the formation of a durable coating with a rather high rutile content ensuring the photocatalytic properties required for its possible use as a protective self-cleaning coating. In this regard, the consumptions of the powder and gas mixture were selected in a manner such that there was a sufficient amount of oxygen to oxidize titanium and achieve the optimal proportion of its oxides in the required fraction. Of primary importance is the fact that the selected composition of the gas mixture ensured the stability of the detonation setup operation and the reproducibility of the properties of the coatings produced under the same conditions.

The adhesion strengths of similar coatings obtained using a similar setup were studied earlier and amounted to, on average, 52–53 MPa [19].

The measurements were carried out for coatings obtained under different regimes, in which the following parameters were varied: distances d between the detonation gun nozzle and the substrate (spraying distance) of 40, 50, 60, 70, and 80 mm and speeds s of detonation gun movement (nozzle speeds) of 400, 800, 1200, 1600, and 2000 mm/min. The studies of the surfaces of the obtained coatings showed that roughness height Rz of their profiles varied in a range of 70–250 μm, while the average height of the surface profile was 139.13 μm for all coatings. Roughness (arithmetic mean deviation of the profile) Ra varied in a range of 12.1–33.6 μm, and its average value was 19.91 μm for all coatings.

Figures 2a and 2b present the optical images (height maps) that visually illustrate the surface morphologies of coatings obtained using the two selected spraying regimes. It is clearly seen that the coatings obtained at different spraying parameters have differ-

(a)

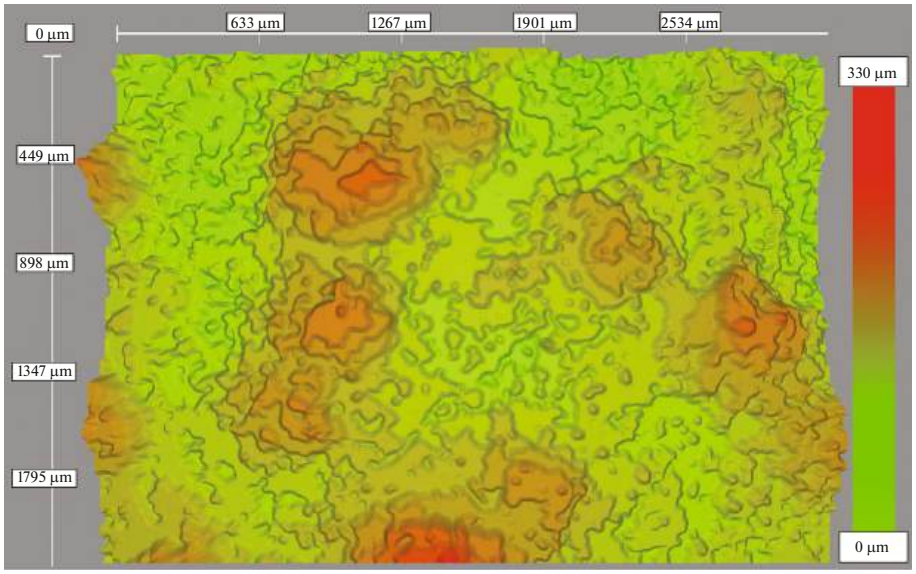

(b)

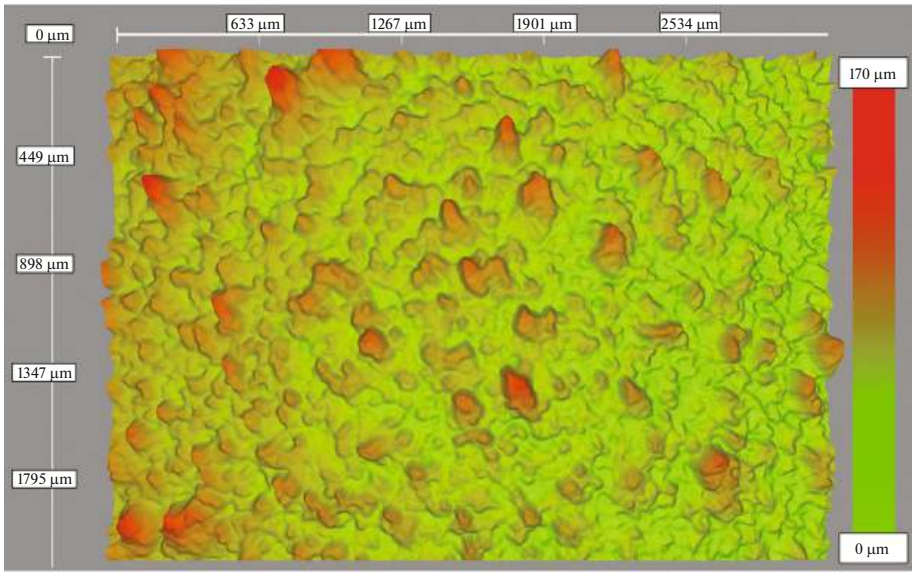

Fig. 2. Optical image of coating surfaces obtained at $d = 40$ mm, $s =$ (a) 400 and (b) 2000 mm/min.

ent morphologies. The height map of the sample obtained at the lowest nozzle speed (Fig. 2a) shows the presence of surface irregularities with diameters of 200–700 μm and heights of 150–330 μm (relative to the minimum height of the coating surface) at specific points, with this finding being relevant to the concentration of the kinetic energy at these points. In turn, the height map of the sample obtained at the highest nozzle speed (Fig. 2b) and the same spraying distance as those for the previous sample shows a uniform distribution of the surface irregularities over the sample area, which is due to the fact that the energy is not concentrated at a point, when the spraying distance is large. As a consequence, the kinetic energy is quasi-uniformly distributed between the powder particles during the spraying process, thus leading to a smoother surface topography of the coating obtained at a higher speed.

The performed observations made it possible to reveal the relationship between the spraying technological parameters and the surface roughness of the manufactured samples. In particular, the roughness of all samples decreased monotonically with increasing nozzle speed (Fig. 3). On average, roughness *Ra* decreased from 30.46 μm at a nozzle speed of 400 mm/min to 13.60 μm at a speed of 2000 mm/min.

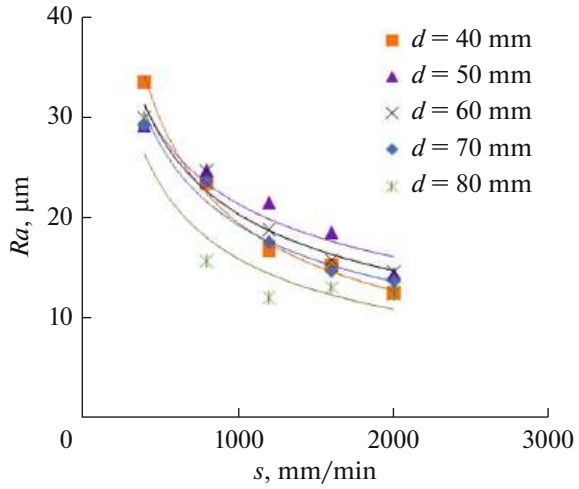

Fig. 3. Dependences of roughness *Ra* (μm) on nozzle speed *s* (mm/min).

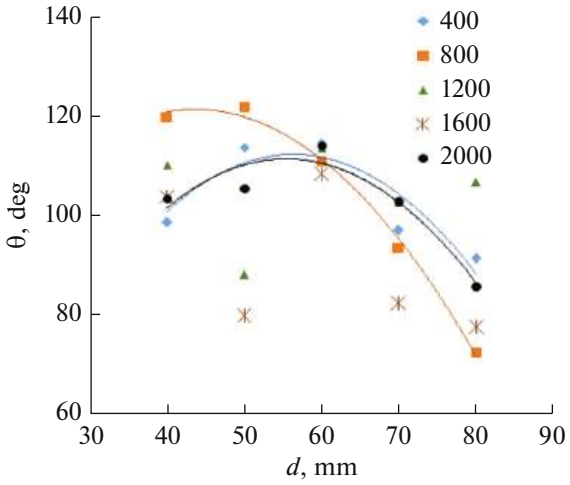

Fig. 4. Dependences of contact angle θ (deg) on spraying distance *d* (mm).

The analysis of the data obtained has shown that the dependence of roughness *Ra* observed in the experiments on nozzle speed *s* obeys the following power law:

$$Ra(s) = \frac{b}{s^p}, \quad (1)$$

where *b* and *p* are empirical coefficients, the values of which, as calculated by the method of least squares, are given in Table 2.

Determination coefficients R^2 of power equation (1) are close to unity, thereby indicating a rather good agreement between the results of observations and the calculated theoretical dependence.

The results of measuring contact angle θ showed that its average value for all coatings was 100.58°; the largest value observed at a spraying distance of 50 mm and a nozzle speed of 800 mm/min was 122.11°, while the lowest value observed at a spraying distance of 80 mm and a nozzle speed of 800 mm/min was 72.66°.

The results of measuring the contact angle as depending on spraying distance *d* in two nozzle speed *s* regimes are presented in Fig. 4. The contact angles increase with increasing spraying distance from 98.38°/120.07° to maximum values of 114.76°/122.11°; then, they decrease to 91.55°/72.55° at movement speeds of 400/800 mm/min, respectively.

It should be noted that cosθ is negative for the overwhelming majority of the samples, while its absolute value initially increases with the nozzle speed; then, it decreases. In some regimes (in particular, at $d = 70$ and 80 mm and $s = 1600$ and 2000 mm/min) and at high speeds and large spraying distances, values of $\cos\theta > 0$ are observed.

It has been found that the experimental dependences of contact angle θ on spraying distance *d* at certain nozzle speeds are adequately approximated by the following parabolic equation:

$$\theta(d) = a_2 d^2 + a_1 d + \theta_0, \quad (2)$$

where θ_0 is a conditional contact angle corresponding to the zero spraying distance $\theta_0 = \theta$ ($d = 0$) and a_1 and a_2 are empirical coefficients.

The parameters of Eq. (2) were obtained by the method of least squares so as to ensure that it most adequately corresponds to the experimental data. Their values are given in Table 3. Determination coefficients R^2 for Eq. (2) are close to unity, thus indicating a rather good agreement between the observed data and the calculated theoretical dependence.

It should be emphasized that the approximation of experimental data by parabolic equation (2) turned out to be applicable only for the nozzle speed values indicated in Table 3 (400, 800, and 2000 mm/min). Moreover, this equation is valid only for the process implemented with our detonation spraying setup and within the range of its technical capabilities when choosing a spraying distance from 40 to 80 mm (obviously, a small deviation (±5 mm) is admissible).

For other values of *s* (1200 and 1800 mm/min), the distribution of the experimental points does not allow us to use a parabolic function of the form (2) because

Table 2. Coefficients of Eq. (1), which describes the dependences of roughness *Ra* on nozzle speed *s* at different spraying distances *d*

d, mm	*b*	*p*	R^2
40	1290	0.60	0.989
50	351	0.40	0.903
60	509	0.46	0.971
70	601	0.49	0.971
80	703	0.54	0.843

Table 3. Coefficients of Eqs. (2) and (3) describing the dependence of the contact angle on spraying distance d

s, mm/min	a_2, deg/mm^2	a_1, deg/mm	θ_0, deg	R^2	θ_m, deg	d_m, mm
400	−0.042	4.824	−23.500	0.806	122.721	44.351
800	−0.037	3.282	49.940	0.994	115.018	57.381
2000	−0.041	4.588	−15.540	0.906	112.812	55.951

of the smallness of the determination coefficients calculated for them ($R^2 < 0.3$). As can be seen in Fig. 4, the scatter of the values for these speeds s is significant at different spraying distances.

However, the data obtained indicate that there are regimes of coating spraying in which close values of the contact angles are obtained. Apparently, they may be considered to be optimal from the viewpoint of ensuring a required hydrophobicity of the produced coatings. Parabolic equation (2) can be used to estimate the parameters necessary for optimizing such a spraying process. In particular, using Eq. (2), one can determine maximum contact angle θ_m and optimal spraying distance d_m, at which this angle is achieved. For this purpose, parabolic dependence (2) should be rewritten as

$$\theta(d) = a_2(d - d_m)^2 + \theta_m, \quad (3)$$

where the characteristics of the optimal spraying process are expressed via the following empirical parameters:

$$\theta_m = \theta_0 - a_1^2/4a_2, \quad d_m = -a_1/2a_2. \quad (4)$$

The parameters of Eq. (3) calculated by Eqs. (4) for the optimal spraying process at the selected nozzle speed are given in Table 3.

Parabolic equation (3) can also be used to estimate the contact angle useful to develop recommendations for controlling the water-repellent properties by selecting the spraying distance when producing coatings by the detonation method.

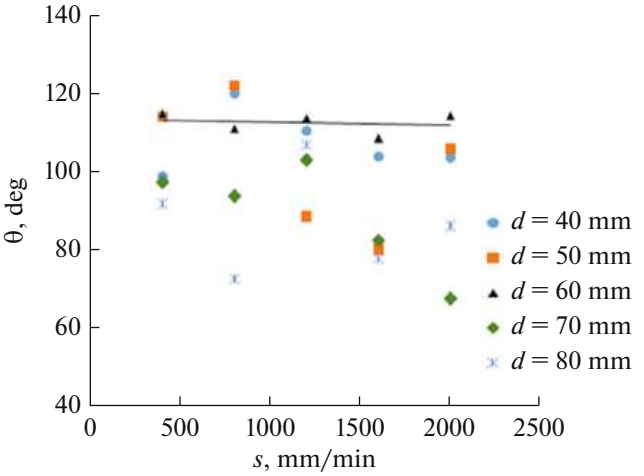

Fig. 5. Distribution of contact angles θ (deg) at different nozzle speeds s (mm/min).

It has been experimentally revealed that, at different spraying distances, the contact angles depend differently on the nozzle speed and are not described by a single dependence. Figure 5 presents the results of measuring the contact angles at coatings obtained at different nozzle speeds. The presented data have shown that the most uniform (constant, i.e., independent of speed s) character of the contact angle distribution is achieved when a spraying distance of 60 mm is selected (straight line parallel to the abscissa axis in Fig. 5). The average contact angle for this spraying distance is 112.49°. It can be seen that these technological parameters are quite close to the theoretically calculated optimal values of the spraying parameters (Table 3).

The results of our experiments have indicated that the surfaces of most coatings are hydrophobic. The hydrophobicity can be increased when producing the coatings by choosing the optimal spraying regime, in which the contact angle reaches its maximum value.

The analysis of the results of measuring the contact angles and roughnesses of the surfaces sprayed under different regimes has made it possible to empirically reveal the existence of a relationship between these parameters (Fig. 6). The contact angle increases as the roughness grows to its average value with respect to the nozzle speeds, which, for spraying distances of 40, 50, and 70 mm, is about 22 μm; then, it decreases with increasing roughness. In particular, the comparison between the values of the roughness and the contact angle at varying nozzle speeds and certain fixed spraying distances (namely, 40, 50, and 70) shows the existence of the following parabolic dependence:

$$\theta(Ra) = \alpha_2 Ra^2 + \alpha_1 Ra + \alpha_0, \quad (5)$$

where α_0 is the conventional contact angle corresponding to the zero roughness, while α_1 and α_2 are empirical coefficients.

Equation (5) allows one to confront the surface roughnesses and the contact angles for the surfaces of coatings obtained under different spraying regimes. The parameters of Eq. (5) were obtained by the method of least squares so that it most adequately corresponded to the experimental data (Table 4).

For Eq. (5), determination coefficients R^2 vary in a range of 0.66–0.86, thereby indicating a satisfactory level of the consistency between the observation results and the calculated theoretical dependence,

since, according to the Chaddock scale, the qualitative characteristic of a relationship is considered to be high at R^2 values ranging from 0.7 to 0.9 [20].

For short spraying distances (40 and 50 mm), $R^2 > 0.8$. Therefore, we may state that, in such spraying regimes, variations in roughness make the greatest contribution as compared with other factors that affect variations in the contact angles and have not been taken into account in Eq. (5). The relationship between the roughness and the contact angle derived under such conditions can be of practical importance.

It should be emphasized that Eq. (5) is applicable only to the spray distances indicated in Table 4 (40, 50, and 70 ± 5 mm). In addition, this equation is valid only when implementing the detonation spraying of coatings with the setup that we used and within the range of its technical capabilities at the chosen nozzle speed within a range of 400–2000 mm/min (obviously, a small deviation ±50 mm/min is admissible), for which roughnesses *Ra* of the manufactured coatings lie in a range of 12–33 μm. For other values of *d* (60 and 80 mm), the distribution of the experimental points makes impossible the use of parabolic Eq. (5) because of the smallness of the determination coefficients calculated for them (therefore, they are not shown in Fig. 4).

It should also be noted that, in our case, the thermophysical features of the detonation spraying process is an indirect factor in determining the contact angle. First of all, this factor affects the phase composition of a coating, while the phase composition affects its other properties [21]. Many studies by both Russian [22, 23] and foreign [24–26] authors have indicated the following significant thermophysical factors of the detonation spraying process. The speed at which the gun is moved along the substrate (nozzle speed) affects the heating of the substrate and the thickness of the coating via the number of shots per unit area. The spraying distance also influences the substrate temperature via the characteristics of the propagation of the detonation gas flow. Filling of the gun with a combustible mixture affects the pressure and temperature of the gas flow and, as a consequence, the chemical transformations in the flying particles being sprayed, as well as the substrate temperature.

In our experiments on the preparation of coatings, the selected composition of the gas mixture, which remained unchanged, made it possible to maintain a constant temperature during the spraying process. Therefore, the temperature factors are not considered in this work.

Series of additional experiments were also carried out to determine the dependence of the size of a sprayed coating spot on the spraying distance. Larger substrates 100 × 100 mm in sizes made of the same St3 steel were used in these experiments. The spraying was carried out at different distances and a fixed nozzle speed of 2000 mm/min. The distribution of the gas flows during the detonation spraying is schematically represented in Fig. 7. The results of these experiments are presented in Table 5 and visualized in Figs. 8 and 9.

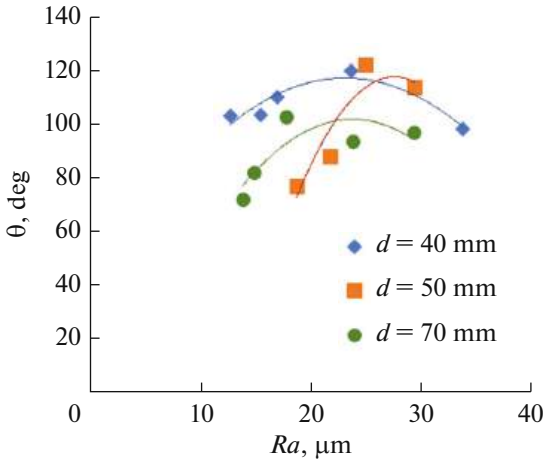

Fig. 6. Relationship between contact angle θ (°) and roughness *Ra* (μm).

Pronounced spots of an approximately circular shape were observed on the large substrates. The sizes of the spots were estimated using the diameters of two zones (Fig. 7, zones *3*, *6*). Red circles in Fig. 7 indicate the spots with diameter D_{cor} formed by the core of the detonation flow (zone *3*). Blue circles indicate spots of partial oxidation with diameter D_{mix}, which are formed by the zone of mixing the detonation flow with atmospheric gases (zone 6). The rest of the sample also has a thin coating that is formed due to the pressure of the turbulent flow. The possibility of such spraying results from the high plasticity of titanium powder.

The diameter of the core of the contact spot varied from 10.14 to 23.74 mm, while its average value was 18.78 mm at all distances. The diameter of the mixing zone spot varied from 35.34 to 69.12 mm, with its average value being 54.95 mm at all distances.

White spots were formed on the samples obtained at distances of 80 mm (Fig. 8d) and 130 mm (Fig. 8f), thus indicating, most likely, the final transformation of oxidized titanium unto the rutile phase. This phenomenon is due to the fact that, at such spraying distances, the substrate is located in the zone of elevated temperatures (Fig. 7, zone *3*) and the titanium powder is oxidized more intensely.

Table 4. Coefficients of Eq. (5), which describes the dependence of the contact angle on spraying distance *d*

d, mm	α_2	α_1	α_0, deg	R^2
40	−0.159	7.347	33.08	0.862
50	−0.568	31.210	−311.10	0.861
70	−0.246	11.690	−36.73	0.662

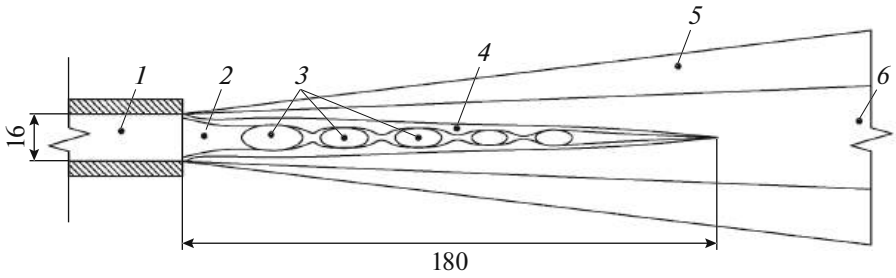

Fig. 7. Schematic representation of the distribution of gas flows during detonation spraying: (*1*) detonation gun nozzle; (*2*) zone of nozzle exit; (*3*) zones of elevated temperatures; (*4*) detonation flow core; (*5*) turbulence zone, and (*6*) zone of mixing with atmospheric gases.

The results of the additional series of experiments have shown that the characteristic diameters of the spots of flow core D_{cor} and mixing zone D_{mix} depend differently on spraying distance d. In particular, the diameter of the mixing zone spot (Fig. 9, curve *1*) monotonically increases with deceleration during spraying at longer distances, while the diameter of the flow core spots (Fig. 9, curve *2*) initially somewhat increases from 19.56 mm to a maximum value of 23.74 mm, at a spraying distance of 80 mm. Then, it begins to decrease rather rapidly to its minimum value with a further increase in the spraying distance.

Note that the dependences of the characteristic spot sizes on the spraying distance are adequately approximated by a parabolic equation. In particular, the dependence of the diameter of the mixing zone is described by parabolic equation $D_{mix}(d) = 29.57 + 0.3748d - 0.00089d^2$ with determination coefficient $R^2 = 0.915$, while the dependence of the diameter of the flow core is described by parabolic equation $D_{cor}(d) = 16.3 + 0.1817d - 0.00139d^2$ with determination coefficient $R^2 = 0.958$ (Fig. 9, solid lines). The determination coefficients are close to unity, with this fact allowing us to believe that the selected equations adequately describe the experimental data within the studied range of the parameters of coating spraying.

Table 5. Results of experimental evaluating the sizes of sprayed spots as depending on the spray distance

Spray distance d, mm	Flow core spot diameter D_{cor}, mm	Mixing zone spot diameter D_{mix}, mm
20	19.56	35.34
40	20.84	42.77
60	21.65	52.31
80	23.74	57.30
100	20.03	50.77
130	15.48	65.54
160	10.14	66.48
200	–	69.12

It is worth noting that the dependence of the diameter of the mixing zone can also be described by logarithmic equation $D_{mix}(d) = 15.05\ln(d/2.065)$ with determination coefficient $R^2 = 0.918$ (Fig. 9, dashed line). It can be seen that the determination coefficient of the logarithmic dependence is slightly higher than that of the parabolic one. However, their difference is very small (0.003), and there is no reason to prefer one curve pattern to another one in the given range of spraying parameters. The logarithmic dependence must correspond to the case of a decelerating monotonic growth as compared with the parabolic dependence, provided that it increases to its maximum. Hence, the choice between these forms of the dependence of the diameter of the mixing zone on the spraying distance can be related to the growth rate of the D_{mix} value with a further increase in d, provided, of course, that the implementation of such coating spraying regimes with the given setup is technically feasible.

CONCLUSIONS

This paper describes the wetting properties of titanium-dioxide-based metal–ceramic coatings as depending on the conditions of their formation by the detonation spraying technology. It has been found that the contact angle and, accordingly, the water-repellent properties of a coating surface can be efficiently controlled by varying the technological parameters of spraying. The spraying distance has the greatest influence on the water-repellent properties of the surfaces of titanium dioxide coatings, while variations in the nozzle speed lead to a uniform distribution of the contact angle values.

The measurements of the surface roughness for the coatings obtained under different conditions have revealed its pronounced dependence on the nozzle speed in accordance with a power law. The proposed

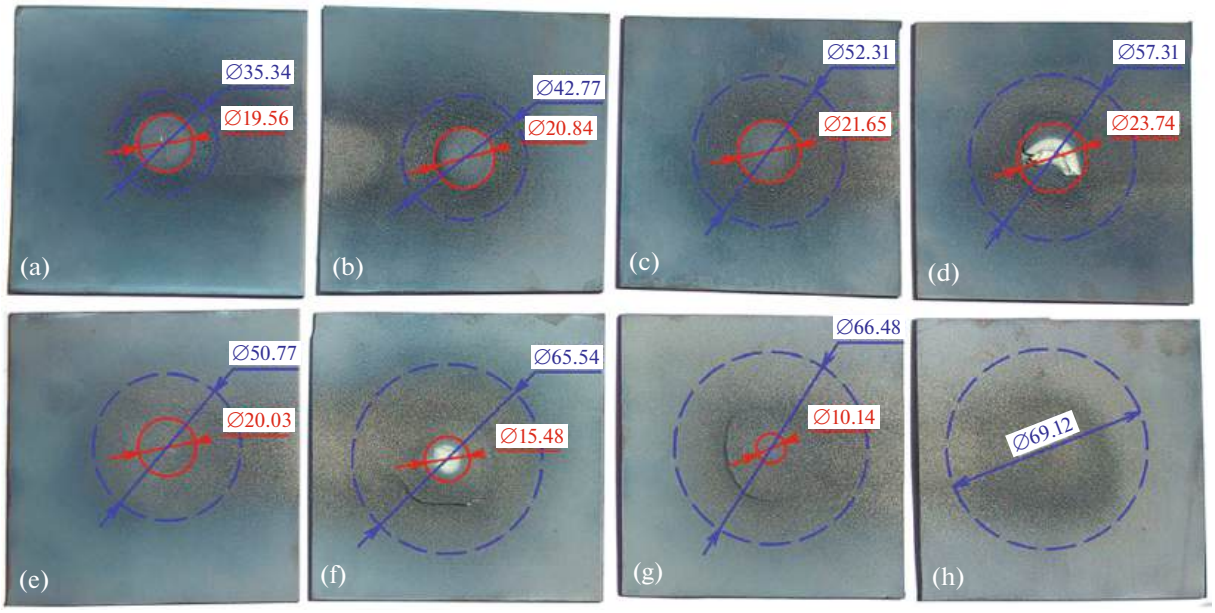

Fig. 8. Samples of coating spots obtained by detonation spraying of titanium powder at different distances from the nozzle (mm): (a) 20, (b) 40, (c) 60, (d) 80, (e) 100, (f) 130, (g) 160, and (h) 200.

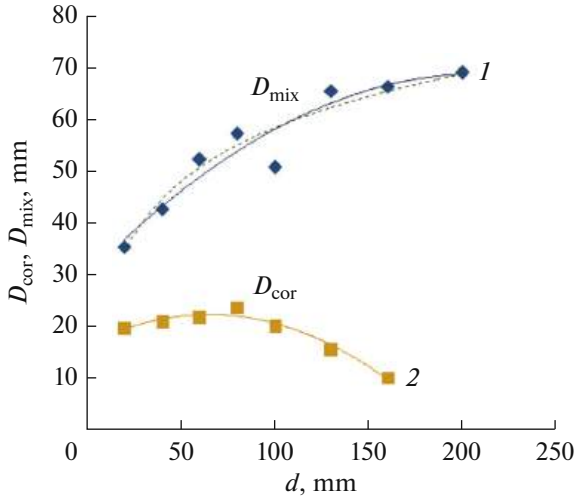

Fig. 9. Dependences of (*1*) mixing zone spot diameter and (*2*) flow core spot diameter on spraying distance (symbols denote experimental data, solid lines refer to approximation by the parabolic equation, and dashed line indicates approximation by the logarithmic equation).

power equation may be useful for predicting the surface roughness of obtained coatings.

It has been inferred from the data of the performed experiments that the dependence of the contact angle on the spraying distance obeys a parabolic law under certain regimes of the detonation setup operation. To describe the experimental data, a phenomenological equation has been proposed that adequately describes the parabolic dependence observed in a number of experiments. The proposed equation may be useful to interpolate (rather than extrapolate) the contact angles within the specified ranges of its applicability. This equation is applicable to determining the optimal regime for spraying coatings, with this regime ensuring the best hydrophobicity of their surfaces.

The experiments have shown that it is possible to determine the optimal values of the technological parameters of detonation spraying that ensure the maximum hydrophobicity of the produced coatings.

The results presented in this article expand the studies of the wetting properties of metal–ceramic coating surfaces and can be used when creating new promising photocatalytic coatings with predictable water-repellent characteristics for protection purposes.

FUNDING

This work was carried out within the framework of the state order of the Ministry of Science and Higher Education of the Russian Federation no. FZWN-2023-0006 using the equipment of the High Technology Center of the Shukhov Belgorod State Technological University and the Joint Research Center “Technologies and Materials” of the Belgorod National Research University.

CONFLICT OF INTEREST

The authors of this work declare that they have no conflicts of interest.

REFERENCES

1. Atacan, K., Güy, N., and Özacar, M., Recent advances in photocatalytic coatings for antimicrobial surfaces, *Curr. Opin. Chem. Eng.*, 2022, vol. 36, no. June, p. 00777. https://doi.org/10.1016/j.coche.2021.100777
2. Obregón, S. and Rodríguez-González, V., Photocatalytic TiO_2 thin films and coatings prepared by sol–gel processing: A brief review, *J. Sol-Gel Sci. Technol.*, 2022, vol. 102, pp. 125–141. https://doi.org/10.1007/s10971-021-05628-5
3. Zhang, W., Gu, J., Zhang, C., Xie, Y., and Zheng, X., Preparation of titania coating by induction suspension plasma spraying for biomedical application, *Surf. Coat. Technol.*, 2019, vol. 358, pp. 511–520. https://doi.org/10.1016/j.surfcoat.2018.11.047
4. Yang, K., Zhong, S., Yue, H., Tang, S., Ma, K., Liu, C., Qiao, K., and Liang, B., Application of pulsed chemical vapor deposition on the SiO_2-coated TiO_2 production within a rotary reactor at room temperature, *Chin. J. Chem. Eng.*, 2022, vol. 45, pp. 22–31. https://doi.org/10.1016/j.cjche.2021.05.012
5. Seremak, W., Baszczuk, A., Jasiorski, M., Gibas, A., and Winnicki, M., Photocatalytic activity enhancement of low-pressure cold-sprayed TiO_2 coatings induced by long-term water vapor exposure, *J. Therm. Spray Technol.*, 2021, vol. 30, pp. 1827–1836. https://doi.org/10.1007/s11666-021-01244-5
6. Islam, M. T., Dominguez, A., Turley, R. S., Kim, H., Sultana, K. A., Shuvo, M. A. I., Alvarado-Tenorio, B., Montes, M. O., Lin, Y., Gardea-Torresdey, J., and Noveron, J. C., Development of photocatalytic paint based on TiO_2 and photopolymer resin for the degradation of organic pollutants in water, *Sci. Total Environ.*, 2020, vol. 704, p. 135406. https://doi.org/10.1016/j.scitotenv.2019.135406
7. Kovaleva, M. G., Prozorova, M. S., Arseenko, M. Yu., Vagina, O. N., and Sirota, V. V., Properties of alumina-titania coating formed by a new multi-chamber gas-dynamic accelerator, *Key Eng. Mater.*, 2017, vol. 753, pp. 117–122. https://doi.org/10.4028/www.scientific.net/KEM.753.117
8. Kovaleva, M., Tyurin, Y., Vasilik, N., Kolisnichenko, O., Prozorova, M., Arseenko, M., Sirota, V., and Pavlenko, I., Structure and microhardness of titanium-based coatings formed by multichamber detonation sprayer, *Phys. Res. Int.*, 2015, vol. 2015, p. 532825. https://doi.org/10.1155/2015/532825
9. Shtertser, A A., Batraev, I.S., Ulianitsky, V.Yu., Kuchumova, I.D., Bulina, N., Ukhina, A., Bokhonov, B.B., Dudina, D., Trinh, P., and Phuong, D.D., Detonation spraying of Ti–Cu mixtures in different atmospheres: Carbon, nitrogen and oxygen uptake by the powders, *Surf. Interfaces*, 2020, vol. 21, p. 100676. https://doi.org/10.1016/j.surfin.2020.100676
10. Liu, Y., Huang, J., Feng, X., and Li, H., Thermal-sprayed photocatalytic coatings for biocidal applications: A review, *J. Therm. Spray Technol.*, 2021, vol. 30, pp. 1–24. https://doi.org/10.1007/s11666-020-01118-2
11. Klochko, N., Klepikova, K., Kopach, V., Khrypunov, G., Myagchenko, Yu., Melnychuk, E., Lyubov, V., and Kopach, A., On controlling the hydrophobicity of nanostructured zinc-oxide layers grown by pulsed electrodeposition, *Semiconductors*, 2016, vol. 50, pp. 352–363. https://doi.org/10.1134/S106378261603012X
12. Zhou, H., Sun, S., and Ding, H., Surface organic modification of TiO_2 powder and relevant characterization, *Adv. Mater. Sci. Eng.*, 2017, vol. 2017, pp. 1–8. https://doi.org/10.1155/2017/9562612
13. Li, Y., Xia, B., and Jiang, B., Thermal-induced durable superhydrophilicity of TiO_2 films with ultra-smooth surfaces, *J. Sol-Gel Sci. Technol.*, 2018, vol. 87, pp. 50–58. https://doi.org/10.1007/s10971-018-4684-0
14. Wu, X. H. and Then, Y. Y., Fabrication and characterization of superhydrophobic graphene/titanium dioxide nanoparticles composite, *Polymers* (Basel), 2021, vol. 14, p. 122. https://doi.org/10.3390/polym14010122
15. Sharifi, N., Pugh, M., Moreau, C., and Dolatabadi, A., Developing hydrophobic and superhydrophobic TiO_2 coatings by plasma spraying, *Surf. Coat. Technol.*, 2016, vol. 289, pp. 29–36. https://doi.org/10.1016/j.surfcoat.2016.01.029
16. Sirota, V. V., Vashchilin, V. S., Ogurtsova, Y. N., Gubareva, E. N., Podgornyi, D. S., and Kovaleva, M. G., Structure and photocatalytic properties of the composite coating fabricated by detonation sprayed Ti powders, *Ceram. Int.*, 2024, vol. 50, pp. 739–749. https://doi.org/10.1016/j.ceramint.2023.10.152
17. Sirota, V. V., Savotchenko, S. E., Strokova, V. V., Vashchilin, V. S., Podgornyi, D. S., Prokhorenkov, D. S., Zaitsev, S. V, and Kovaleva, M. G., Effect of detonation spray regimes on photocatalytic activity of Ti–TiO_2 coatings, *J. Photochem. Photobiol., A*, 2024, vol. 452, p. 115626. https://doi.org/10.1016/j.jphotochem.2024.115626
18. Sirota, V. V., Savotchenko, S. E., Strokova, V. V., Vashchilin, V. S., Podgornyi, D. S., Limarenko, M. V., and Kovaleva, M. G., Effect of irradiation intensity on the rate of photocatalysis of TiO_2 coatings obtained by detonation spraying, *Int. J. Appl. Ceram. Technol.*, 2024, vol. 21. https://doi.org/10.1111/ijac.14782
19. Kovaleva, M., Tyurin, Y., Kolisnichenko, O., Prozorova, M., and Arseenko, M., Properties of detonation nanostructured titanium-based coatings, *J. Therm. Spray Technol.*, 2013, vol. 22, pp. 518–524. https://doi.org/10.1007/s11666-013-9909-8
20. Nikitina, M. A. and Chernukha, I. M., Nonparametric statistics. Part 3. Correlation coefficients, *Theory and Practice of Meat Processing*, 2023, vol. 8, pp. 237–251. https://doi.org/10.21323/2414-438X-2023-8-3-237-251
21. Okamoto, H., O-Ti (Oxygen-titanium), *J. Phase Equilib. Diffus.*, 2011, vol. 32, pp. 473–474. https://doi.org/10.1007/s11669-011-9935-5

22. Dudina, D.V., Zlobin, S.B., Ulianitsky, V.Yu., Lomovsky, O.I., Bulina, N.V., Bataev, I.A., and Bataev, V.A., Detonation spraying of TiO_2–Ag: Controlling the phase composition and microstructure of the coatings, *Ceram. Trans.*, 2012, vol. 237, pp. 161–169. https://doi.org/10.1002/9781118511466.ch17

23. Rakhadilov, B., Buitkenov, D., Sagdoldina, Z., Seitov, B., Kurbanbekov, S., and Adilkanova, M., Structural features and tribological properties of detonation gun sprayed Ti–Si–C coating, *Coatings*, 2021, vol. 11, p. 141. https://doi.org/10.3390/coatings11020141

24. Kantay, N., Rakhadilov, B., Kurbanbekov, S., Yeskermessov, D., Yerbolatova, G., and Apsezhanova, A., Influence of detonation-spraying parameters on the phase composition and tribological properties of Al_2O_3 coatings, *Coatings*, 2021, vol. 11, p. 793. https://doi.org/10.3390/coatings11070793

25. Du, H., Hua, W., Liu, J., Gong, J., Sun, C., and Wen, L., Influence of process variables on the qualities of detonation gun sprayed WC-Co coatings, *Mater. Sci. Eng., A*, 2005, vol. 408, pp. 202–210. https://doi.org/10.1016/j.msea.2005.08.008

26. Senderowski, C. and Bojar, Z., Influence of detonation gun spraying conditions on the quality of Fe-Al intermetallic protective coatings in the presence of NiAl and NiCr interlayers, *J. Therm. Spray Technol.*, 2009, vol. 18, pp. 435–447. https://doi.org/10.1007/s11666-009-9328-z